

PDF hosted at the Radboud Repository of the Radboud University Nijmegen

The following full text is a publisher's version.

For additional information about this publication click this link.

<http://hdl.handle.net/2066/99078>

Please be advised that this information was generated on 2019-02-24 and may be subject to change.

Communications: The structure of Rh_8^+ in the gas phase

D. J. Harding,^{1,a)} T. R. Walsh,² S. M. Hamilton,³ W. S. Hopkins,³ S. R. Mackenzie,³ P. Gruene,⁴ M. Haertelt,⁴ G. Meijer,⁴ and A. Fielicke^{4,b)}

¹Department of Chemistry, University of Warwick, Coventry CV4 7AL, United Kingdom

²Department of Chemistry and Centre for Scientific Computing, University of Warwick, Coventry CV4 7AL, United Kingdom

³Department of Chemistry, Physical and Theoretical Chemistry Laboratory, University of Oxford, South Parks Road, Oxford OX1 3QZ, United Kingdom

⁴Fritz-Haber-Institut der Max-Planck-Gesellschaft, Faradayweg 4-6, Berlin D-14195, Germany

(Received 26 September 2009; accepted 14 December 2009; published online 6 January 2010)

The geometric structure of the Rh_8^+ cation is investigated using a combination of far-infrared multiple photon dissociation spectroscopy and density functional theory (DFT) calculations. The energetic ordering of the different structural motifs is found to depend sensitively on the choice of pure or hybrid exchange functionals. Comparison of experimental and calculated spectra suggests the cluster to have a close-packed, bicapped octahedral structure, in contrast to recent predictions of a cubic structure for the neutral cluster. Our findings demonstrate the importance of including some exact exchange contributions in the DFT calculations, via hybrid functionals, when applied to rhodium clusters, and cast doubt on the application of pure functionals for late transition metal clusters in general. © 2010 American Institute of Physics. [doi:10.1063/1.3285266]

The study of transition metal (TM) clusters offers the opportunity to probe the fundamental physics involved in the transition from atomic to bulk properties¹ and a means to better understand potentially tractable model systems for supported catalysts.² A wide range of cluster properties, including reactivity,^{3,4} magnetic moments,^{5,6} electric polarizability,⁷ and ionization potential^{8,9} have been found to depend sensitively, and nonmonotonically, on cluster size. These size effects reflect the complex evolution of the electronic and geometric structures and yet, the structures of most of these clusters are not currently known.

Although knowledge of cluster structures is vital for developing a deeper understanding of the observed properties, experimental structure determination in the gas phase remains difficult. Photoelectron spectroscopy has been applied to anionic clusters and has yielded detailed information on the size-dependent evolution of electronic structures.¹⁰ Only in the past few years, however, has it become possible to probe more directly the geometric structures of TM clusters in the gas phase, e.g., by measuring their ion mobilities,¹¹ by trapped ion electron diffraction,¹² or far-infrared multiple photon dissociation (FIR-MPD) spectroscopy.¹³

Theory has been widely used to predict the geometric and electronic structures of clusters. Electronic structure theory is a vital aid to experimental efforts to determine cluster structure¹¹⁻¹⁴ and to help understand the effects of structure on cluster properties.^{15,16} The large size of TM clusters, both in terms of the number of electrons which must be treated and the complexity of the potential energy surfaces (PESs), generally restricts practical calculations to the realm

of DFT. Application of DFT to mid-sized TM clusters requires caution in the interpretation of results; not only because of the approximations inherent to all contemporary exchange-correlation functionals but also because there is a lack of benchmark data from high-quality multireference electronic structure theory, although data do exist for rhodium clusters as large as the pentamer.¹⁷ Most contemporary functionals were not designed with TM clusters in mind and it is not clear if one single exchange-correlation functional is to be preferred for all TM clusters.

Rhodium clusters present many of these challenges and opportunities and, as a consequence, have been studied experimentally in some detail.^{3-5,7} This work represents the first direct measurements of their structure. Recent DFT calculations have predicted a range of unusual putative global minimum and low-energy structures for rhodium clusters,^{15,18-21} which are not based on the close-packed motifs identified for many TM clusters.^{14,22,23} These include a trigonal prism for Rh_6 (Ref. 19) and Rh_6^+ (Ref. 15) and a cubic structure for Rh_8 .¹⁸⁻²⁰ Cubic motifs have also been reported for larger clusters.^{20,21} Cube-based structures have been rationalized by strong *d*-orbital character in the bonding, favoring 90° bond angles and eight-center bonding.²⁰ These structures are qualitatively different to the close-packed, polytetrahedral structures reported for most cluster sizes by Futschek *et al.*²⁴ As the computational methods used in these studies are rather similar, all using DFT, it is not clear if the differences in the results are due to the range of structures and motifs considered for each cluster size or due to differences in the details of the calculations, such as the exchange-correlation functionals used.

Cubic structures have also been predicted for other platinum group metals including ruthenium.^{25,26} For this metal, Wang and Johnson²⁷ have investigated in detail the effects of

^{a)}Present address: Fritz-Haber-Institut der Max-Planck-Gesellschaft, Faradayweg 4-6, D-14195 Berlin, Germany.

^{b)}Electronic mail: fielicke@fhi-berlin.mpg.de.

using pure and hybrid functionals on the favored geometry of small ($n \leq 4$) clusters. They reported that while pure functionals predicted a square planar isomer as global minimum for Ru_4 , hybrid functionals favored a tetrahedral isomer. They attributed the difference to changes in the relative energy of the s and d orbitals in the ruthenium atom. The proximity of rhodium and ruthenium in the periodic table suggested similar effects may be observed for rhodium clusters, supported by the recent results of Sun *et al.*²¹ Experiments which allow a direct comparison between the experimental results and calculated properties therefore provide a vital means to test and benchmark the theoretical methods used to study these systems. Here, we focus on structure determination for the archetypal cubic cluster, Rh_8^+ , by gas-phase vibrational spectroscopy. An eight-atom cluster is the smallest cluster which can form a complete cube and therefore provides an ideal candidate system to test the competition between cubic and close-packed geometries. IR spectroscopy is particularly sensitive to symmetry through its selection rules which, for an eight-atom cube, predict a single triply degenerate IR-active mode of t_{1u} symmetry.

FIR-MPD allows the measurement of size-specific IR spectra of clusters in the gas phase, which can be compared to the results of calculations. The technique has been described in detail previously.¹³ As implemented here, argon-tagged rhodium cluster cations are formed by laser ablation of a rotating rhodium metal target. The resulting plasma is cooled by a mixed pulse of helium and argon (ca. 0.3%) and carried down a cryogenically cooled clustering channel (173 K) before expansion into vacuum. The resulting cluster beam passes through a skimmer before entering the FIR laser interaction region, where it is intersected by a counterpropagating beam from the Free Electron Laser for Infrared eXperiments (FELIX). By recording time-of-flight mass spectra alternately with and without FELIX irradiation, the depletion of Ar-tagged clusters can be measured as a function of IR wavelength. From this, the size-specific absorption spectra are obtained as described before.¹³

The experimental FIR-MPD spectrum of Rh_8Ar^+ is shown in the lower panel of Fig. 1. It appears relatively simple, having an intense peak at $206 \pm 1 \text{ cm}^{-1}$ and a smaller peak at $250 \pm 1 \text{ cm}^{-1}$. The spectrum of Rh_8Ar_2^+ is very similar, showing no large changes in peak position or intensity with the degree of argon coverage. This indicates that the Ar acts as spectator and is not influencing the cluster structures. This is consistent with the findings, e.g., for the larger cobalt clusters.²⁸

In order to determine the structure of the clusters, the experimental FIR-MPD spectra are compared with calculated vibrational spectra. A thorough search of the PES has been performed in order to identify the important, i.e., low-energy, geometric structures of the cluster. We have used a two-stage approach; first employing basin-hopping (BH) simulations²⁹ to locate candidate structures, and second by refining these candidate structures. In the first stage, we used BH in two different implementations; the first using the Sutton–Chen³⁰ model potential, and the second based on the PES described by the local density approximation.^{31,32} In addition to the structures found in our BH simulations, a range of previously

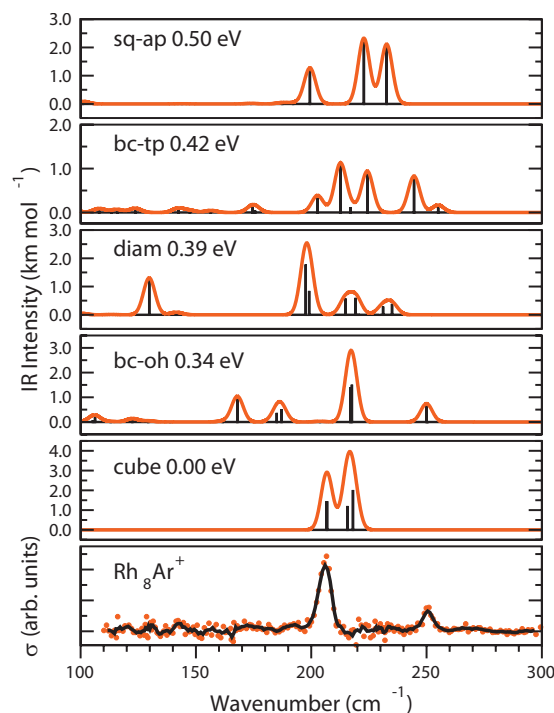


FIG. 1. Predicted IR spectra of Rh_8^+ from pure (PBE) DFT calculations compared to the experimental FIR-MPD spectrum of Rh_8Ar^+ . σ is the experimental IR cross section. The labels correspond to the structures shown in Fig. 2.

reported structures were also investigated.^{19,20,24} In the second stage all the candidate structures were further optimized using DFT, performed with the GAUSSIAN03 package.³³ Perdew, Becke, and Ernzerhof's pure PBE (Ref. 34) and the hybrid PBE1 (25% Hartree–Fock exchange)^{34,35} exchange-correlation functionals were used, allowing a direct comparison of the inclusion of partially exact exchange. The proportion of HF exchange in PBE1 was suggested by Perdew *et al.*,³⁵ on the basis of perturbation theory, to provide the best single choice for a range of systems. The lanl2dz relativistic effective core potentials and basis sets³⁶ were employed. A range of spin-multiplicities were considered in order to determine the favored spin state for each isomer and functional. The cluster symmetry was not constrained. All the optimized structures featured C_1 symmetry, showing small distortions from their higher-symmetry counterparts. Analytic frequency calculations were performed to ensure the structures to be true local minima at each level of theory and to provide comparison with the FIR-MPD spectra. The calculated frequencies are not scaled. Test calculations at the PBE1/lanl2dz level for the neutral dimer give a frequency of 304.5 cm^{-1} for the $^5\Sigma_u$ electronic state, close to the experimental value of $283.9(18) \text{ cm}^{-1}$ that has been obtained from matrix isolation resonance Raman spectroscopy.³⁷ Given the difficulties experienced by current DFT methods in TM dimer systems with significant multiconfigurational character³⁸ – a group which includes Rh_2 ^{39,40} – one has to be careful with this comparison. However, in similar cases such comparisons have been used to obtain an optimal scaling factor²³ and we now take it as an indication that the factor to be used here will be close to unity. To aid comparison, the calculated stick spectra were broadened by a Gaussian line

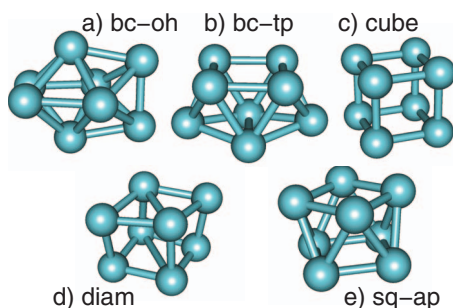


FIG. 2. Geometric structures of low-energy isomers of Rh_8^+ identified in DFT calculations: (a) bicapped octahedron (bc-oh), (b) bicapped trigonal prism (bc-tp), (c) cube, (d) diamond prism (diam), (e) square antiprism (sq-ap).

shape function with a full width at half maximum height of 6 cm^{-1} . The calculations were performed without explicit consideration of the argon tagging atoms as the experimental spectra were not found to depend significantly on the degree of argon coverage.

The results of the calculations are summarized in Fig. 2 which shows the most important geometric structures and in Table I where the relative energies of the favored spin multiplicity of each isomer at the pure and hybrid levels are listed. The Cartesian coordinates of the different isomers and a list of total energies as a function of the total spin multiplicity are available in the supplementary information.⁴¹ We find there to be a significant difference in the energy ordering of the isomers at the two levels. At the pure level, the cube is the lowest-energy structure followed by the bicapped octahedron, broadly in agreement with the results reported by Bae *et al.*¹⁹ for the neutral clusters. At the hybrid level, however, the bicapped octahedron is favored, followed by the bicapped trigonal prism. The cube isomer is supported at the hybrid level but is relatively high in energy (0.92 eV). The favored spin multiplicities for each isomer are generally higher at the hybrid level, a point previously noted by Wang and Johnson.²⁷ This is particularly evident for the cube, for which the pure functional favors an octet while the hybrid favors a 12-tet. A large number of unpaired electrons is generally in agreement with the experimental finding of magnetic moments of up to $0.8 \pm 0.2 \mu_B$ per atom for small neutral rhodium clusters.⁵ The structures optimized at the PBE1 level, particularly for the bicapped octahedron and cube isomers, are significantly less distorted than those at the PBE level, which is in turn visible in the calculated IR spectra.

TABLE I. Relative energies and favored spin multiplicities of different isomers of Rh_8^+ at pure and hybrid levels of theory.

Isomer	Pure functional (PBE)		Hybrid functional (PBE1)	
	2S+1	Relative energy (eV)	2S+1	Relative energy (eV)
cube	8	0.00	12	0.92
bc-oh	14	0.34	14	0.00
diam	12	0.39	^a	^a
bc-tp	10	0.42	14	0.18
sq-ap	10	0.50	12	0.56

^aStructure collapsed during optimization.

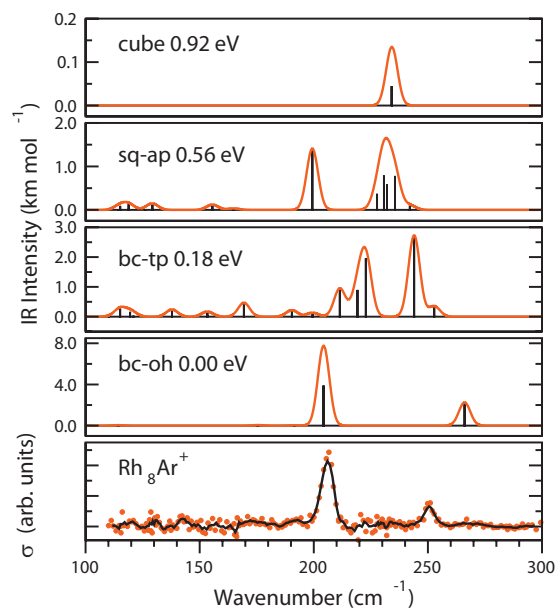


FIG. 3. Predicted IR spectra of Rh_8^+ from hybrid (PBE1) DFT calculations compared to the experimental FIR-MPD spectrum of Rh_8Ar^+ . The labels correspond to the structures shown in Fig. 2.

For ruthenium, significant differences between pure and hybrid DFT emerge in the predicted energetic ordering of the occupied orbitals of the atom.²⁷ However, for rhodium we do not observe such changes, making it more difficult to explain the underlying cause of the differences in the pure and hybrid calculations.

In Figs. 1 and 3 we compare the experimental FIR-MPD spectrum of Rh_8Ar^+ with the calculated spectra from pure and hybrid calculations, respectively. Comparison of the experimental spectrum with calculated spectra at the pure level shows poor agreement with the spectrum of the cubic isomer. For this, three rather closely spaced IR-active modes are predicted at ca. 205 cm^{-1} but no features in the region of 250 cm^{-1} .

A similar comparison with the spectra calculated at the hybrid level shows the experimental spectrum to be well reproduced, both in position and relative intensity, by the lowest-energy bicapped octahedron isomer. This has an intense feature at 205 cm^{-1} and a weaker feature at 266 cm^{-1} , blueshifted by 15 cm^{-1} compared to the experimental spectrum. It is notable that among the different isomers at the pure level the best match to experiment is also provided by the bicapped octahedron, though in this case extra features are predicted at low wavenumber. The calculated spectra of the other isomers at the hybrid level do not provide a good match to experiment, having too few or too many features. The spectrum of the cubic isomer is calculated to have a triply degenerate feature of very low oscillator strength at 234 cm^{-1} , half way between the two features observed experimentally.

The combination of observed vibrational spectra and calculations based on the hybrid PBE1 functional strongly suggest that the Rh_8^+ cluster favors a close-packed, bicapped octahedron structure and not a cubic structure as has been previously reported, and indicated by our own DFT calculations based on the pure PBE functional. In the absence of

high-level multireference benchmark calculations, our findings cast doubt over the suitability of pure functionals when applied to small/midsized late TM clusters. Our evidence, while specific to Rh_8^+ , suggests in general that the expectation of open structures such as those based on cubic motifs in a range of late TM cluster sizes may be misconceived. Further evidence, comprising close comparison of experiment and theory for other sizes of Rh clusters and other metals will be required to resolve this question.

ACKNOWLEDGMENTS

We gratefully acknowledge the support of the Warwick Centre for Scientific Computing for computer time and the Stichting voor Fundamenteel Onderzoek der Materie (FOM) for providing beam time on FELIX. The authors thank the FELIX staff for their skillful assistance, in particular Dr. B. Redlich and Dr. A.F.G. van der Meer. We thank Dr. David Rayner for providing the rhodium rod. This work is supported by the Cluster of Excellence “Unifying Concepts in Catalysis” coordinated by the Technische Universität Berlin and funded by the Deutsche Forschungsgemeinschaft. DJH acknowledges an Early Career Fellowship from the Institute of Advanced Study, University of Warwick, SRM an Advanced Research Fellowship from the EPSRC and WSH the support of the Ramsay Memorial Fellowship Trust.

¹F. Baletto and R. Ferrando, *Rev. Mod. Phys.* **77**, 371 (2005).

²M. Knickelbein, *Annu. Rev. Phys. Chem.* **50**, 79 (1999).

³C. Adlhart and E. Uggerud, *J. Chem. Phys.* **123**, 214709 (2005).

⁴D. Harding, M. S. Ford, T. R. Walsh, and S. R. Mackenzie, *Phys. Chem. Chem. Phys.* **9**, 2130 (2007).

⁵A. J. Cox, J. G. Louderback, S. E. Apsel, and L. A. Bloomfield, *Phys. Rev. B* **49**, 12295 (1994).

⁶F. W. Payne, W. Jiang, and L. A. Bloomfield, *Phys. Rev. Lett.* **97**, 193401 (2006).

⁷M. K. Beyer and M. B. Knickelbein, *J. Chem. Phys.* **126**, 104301 (2007).

⁸M. B. Knickelbein and S. Yang, *J. Chem. Phys.* **93**, 5760 (1990).

⁹M. B. Knickelbein, *Phys. Rev. A* **67**, 013202 (2003).

¹⁰H. Wu, S. R. Desai, and L.-S. Wang, *Phys. Rev. Lett.* **77**, 2436 (1996).

¹¹S. Gilb, P. Weis, F. Furcher, R. Ahlrichs, and M. M. Kappes, *J. Chem. Phys.* **116**, 4094 (2002).

¹²D. Schooss, M. N. Blom, J. H. Parks, B. v. Issendorff, H. Haberland, and M. M. Kappes, *Nano Lett.* **5**, 1972 (2005).

¹³A. Fielicke, A. Kirilyuk, C. Ratsch, J. Behler, M. Scheffler, G. von Helden, and G. Meijer, *Phys. Rev. Lett.* **93**, 023401 (2004).

¹⁴P. Gruene, D. M. Rayner, B. Redlich, A. F. G. van der Meer, J. T. Lyon, G. Meijer, and A. Fielicke, *Science* **321**, 674 (2008).

¹⁵D. Harding, S. R. Mackenzie, and T. R. Walsh, *J. Phys. Chem. B* **110**, 18272 (2006).

¹⁶H. Grönbeck, A. Hellman, and A. Gavrin, *J. Phys. Chem. A* **111**, 6062 (2007).

¹⁷D. Majumdar and K. Balasubramanian, *J. Chem. Phys.* **108**, 2495 (1998).

¹⁸W. Zhang, L. Xiao, Y. Hirata, T. Pawluk, and L. Wang, *Chem. Phys. Lett.* **383**, 67 (2004).

¹⁹Y.-C. Bae, H. Osanai, V. Kumar, and Y. Kawazoe, *Phys. Rev. B* **70**, 195413 (2004).

²⁰Y.-C. Bae, V. Kumar, H. Osanai, and Y. Kawazoe, *Phys. Rev. B* **72**, 125427 (2005).

²¹Y. Sun, R. Fournier, and M. Zhang, *Phys. Rev. A* **79**, 043202 (2009).

²²C. Ratsch, A. Fielicke, A. Kirilyuk, J. Behler, G. von Helden, G. Meijer, and M. Scheffler, *J. Chem. Phys.* **122**, 124302 (2005).

²³A. Fielicke, C. Ratsch, G. von Helden, and G. Meijer, *J. Chem. Phys.* **127**, 234306 (2007).

²⁴T. Futschek, M. Marsman, and J. Hafner, *J. Phys.: Condens. Matter* **17**, 5927 (2005).

²⁵W. Zhang, H. Zhao, and L. Wang, *J. Phys. Chem. B* **108**, 2140 (2004).

²⁶S. Li, H. Li, J. Liu, X. Xue, Y. Tian, H. He, and Y. Jia, *Phys. Rev. B* **76**, 045410 (2007).

²⁷L.-L. Wang and D. Johnson, *J. Phys. Chem. B* **109**, 23113 (2005).

²⁸R. Gehrke, P. Gruene, A. Fielicke, G. Meijer, and K. Reuter, *J. Chem. Phys.* **130**, 034306 (2009).

²⁹D. J. Wales and J. P. K. Doye, *J. Phys. Chem. A* **101**, 5111 (1997).

³⁰A. P. Sutton and J. Chen, *Philos. Mag. Lett.* **61**, 139 (1990).

³¹J. C. Slater, *Phys. Rev.* **81**, 385 (1951).

³²S. H. Vosko, L. Wilk, and M. Nusair, *Can. J. Phys.* **58**, 1200 (1980).

³³M. J. Frisch, G. W. Trucks, H. B. Schlegel, G. E. Scuseria, M. A. Robb, J. R. Cheeseman, J. T. V. J. A. Montgomery, K. N. Kudin, J. C. Burant, J. M. Millam *et al.* (Gaussian, Inc., Pittsburgh, 2003).

³⁴J. P. Perdew, K. Burke, and M. Ernzerhof, *Phys. Rev. Lett.* **77**, 3865 (1996).

³⁵J. P. Perdew, M. Ernzerhof, and K. Burke, *J. Chem. Phys.* **105**, 9982 (1996).

³⁶P. J. Hay and W. R. Wadt, *J. Chem. Phys.* **82**, 270 (1985).

³⁷H. Wang, H. Haouari, R. Craig, Y. Liu, J. R. Lombardi, and D. M. Lindsay, *J. Chem. Phys.* **106**, 2101 (1997).

³⁸N. E. Schultz, Y. Zhao, and D. G. Truhlar, *J. Phys. Chem. A* **109**, 4388 (2005).

³⁹F. Illas, J. Rubio, J. Cañellas, and J. M. Ricart, *J. Chem. Phys.* **93**, 2603 (1990).

⁴⁰K. Balasubramanian and D. W. Liao, *J. Phys. Chem.* **93**, 3989 (1989).

⁴¹See supplementary material at <http://dx.doi.org/10.1063/1.3285266> for details of the quantum chemical calculations.